2013 SNMMI Highlights Lecture: Oncology

From the Newsline Editor: The Highlights Lecture, presented at the closing session of each SNMMI Annual Meeting, was originated and presented for more than 33 y by Henry N. Wagner, Jr., MD. Beginning in 2010, the duties of summarizing selected significant presentations at the meeting were divided annually among 4 distinguished nuclear and molecular medicine subject matter experts. The 2013 Highlights Lectures were delivered on June 12 at the SNMMI Annual Meeting in Vancouver, British Columbia. The final presentation is included here (the first appeared in the September Newsline and the second and third in the October issue). Richard L. Wahl, MD, spoke on oncology highlights. Note that in the following presentation summary, numerals in brackets represent abstract numbers as published in The Journal of Nuclear Medicine *(2013;55[suppl 2]).*

As in years past, oncology was a major focus at the SNMMI 2013 Annual Meeting. In addition to 532 clinical and basic science oncology-related abstracts, special sessions on instrumentation and on molecular targeting probes accounted for more than 500 additional abstracts with relevance in oncology. The result was more than 1,000 candidates for inclusion in this highlights presentation. Many authors generously provided slides from their lectures and exhibits, with far too many excellent projects to include in this time-limited review.

We were reminded once again this year that this is indeed an international meeting, with presenters from 38 countries reporting on oncology topics. The United States was the largest contributor of abstracts, but Korea, China, and Japan, as well as Germany, France, Italy, and the United Kingdom, were also well represented.

In Dr. Bengel's Cardiac Highlights Lecture we heard that PET clearly dominated SPECT at this meeting, and this is also true for oncology. More than 90% of the oncology presentations focused on PET. Diagnosis remains important, as well as monitoring in therapy. Although we are moving toward a greater focus on treatment, we do not yet see as many presentations on treatment as we are likely to see in the future.

Our most used tracer remains ^{18}F-FDG, which has a wide lead over newer ^{18}F-labeled agents. ^{11}C, although obviously useful in a number of settings, is not yet frequently applied and was the focus of far fewer presentations than ^{18}F-labeled agents.

Oncologic imaging is composed of a number of constituent building blocks, and I have structured this talk to reflect these areas, each of which contributes to dynamic growth and continued exploration in nuclear medicine oncology. We need imaging probes that elucidate key biologic elements, including improvements in imaging devices, image analysis, and quantitation to extract the information necessary to make decisions in an objective manner. We can then apply these in diagnosis and staging and for therapy and guidance, all of which have the potential to lead to beneficial changes in management. We also must continue to address the need for comparative effectiveness research so that we can justify the cost and effort involved in our procedures.

Imaging Probes

Our focus has long been on radioactive probes, but optical probes are also an area of increasing promise for large numbers of investigators. Presentations at the meeting also looked at specialized MR imaging probes. In addition, development of multifunctional probes, including nanoprobes, is moving rapidly from in vitro to in vivo applications.

Richard L. Wahl, MD

Dzandzi et al. from McMaster University (Hamilton, Canada) reported on "A hybrid solution-solid-phase kit-type radioiodination and purification platform" [495]. This kit was designed to produce iodine-based radiopharmaceuticals in high yield and incorporates in situ (non–high performance liquid chromatography–based) purification. Successful versions of this kit might provide access to iodine-based radiopharmaceuticals in parts of the world in which they were previously unavailable. The authors showed that they could synthesize, purify, and formulate ^{131}I-metaiodobenzylguanidine and ^{131}I-iododeoxyuridine, for example, in <30 minutes at room temperature.

We are all familiar with DOTA and its importance in chelating metals, but other chelators are being explored. Price et al. from the University of British Columbia (Vancouver, Canada), TRIUMF (Vancouver, Canada), and the Memorial Sloan–Kettering Cancer Center (New York, NY) reported on "H_4octapa-trastuzumab: a versatile acyclic chelator-immunoconjugate with superior properties to DOTA for ^{111}In/^{177}Lu imaging and therapy" [500]. Figure 1 shows excellent results in animals. The advantages of this approach could include faster labeling (<15 min) with a better yield at lower temperatures than required for DOTA. This could result in easier labeling of more biologically susceptible carriers.

Waldron et al. from the University of Mainz (Germany) and Durham University (UK) reported on "Novel chelators for ^{68}Ga PET" [497]. Among the chelators this group described was the DATA chelator, which could be labeled at a pH of 3.7–7 at room temperature in <3 minutes, in contrast to DOTA at 95°C and 10 min. Some compounds simply cannot be labeled at the high temperatures required by DOTA, so these new chelators offer opportunities for broadening the spectrum of biologics and peptides that can be labeled as PET tracers.

An interesting tracer binding agent against neurotensin was described by Wu et al. from the Beckman Research Institute of the City of Hope (Duarte, CA) and the University of Southern California (Los Angeles, CA), who reported

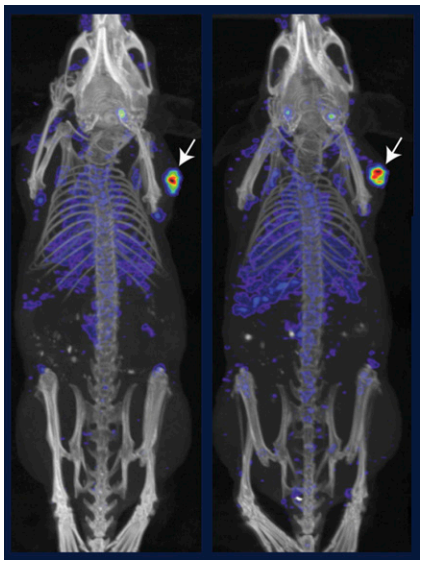

FIGURE 1. Preclinical images with acyclic chelator–immunoconjugate H_4octapa-trastuzumab labeled with ^{111}In (left) and ^{177}Lu (right).

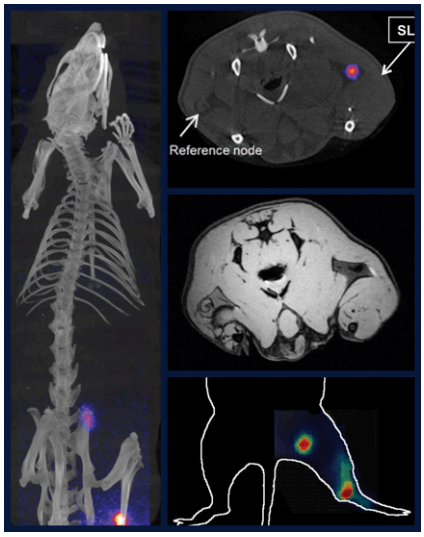

FIGURE 3. Representative images of sentinel lymph nodes (SLN) in rats injected with ^{68}Ga-labeled superparamagnetic nanoparticles for multiple PET, MR, and Cherenkov luminescence imaging (CLI). PET images (left and middle left) are for easy identification of the SLN. MR images (middle right) are for in vivo diagnostic purposes, and the CLI (right) is for intraoperative SLN identification. Images were acquired 3 hours after injection.

on "Evaluation of ^{18}F-DEG-VS-NT as a PET probe for neurotensin receptor-1 targeted imaging" [220]. In animal studies (Fig. 2) neurotensin receptor-1 appeared to have a fair degree of specificity in certain types of tumors, and the in vivo biodistribution at 2 hours after injection was quite impressive. Small molecules often have high uptake in the kidneys, but this agent had high targeting in tumor with low renal uptake. These results are encouraging and suggest that this agent may in time become clinically useful in oncology imaging.

We saw several examples at the SNMMI 2013 meeting of multifunctional or multiparametric agents. Madru et al. from Lund University (Sweden) reported on "^{68}Ga-labeled superparamagnetic nanoparticles for multiple PET/MR/Cherenkov luminescence imaging of sentinel nodes" [4]. Figure 3 shows PET/CT, MR, and Cherenkov luminescence imaging of a sentinel lymph node (SLN) in an animal model. Another approach was described by Thorek et al. from the Memorial Sloan–Kettering Cancer Center (New York, NY), who reported on "^{89}Zr-ferumoxytol iron oxide nanoparticles for multimodality PET/MR lymph node mapping" [6]. Figure 4 shows nodes in the periaortic region of an animal on PET/CT, with signal deficit on the MR image. The results allow for intraoperative guidance and confirmation of resection.

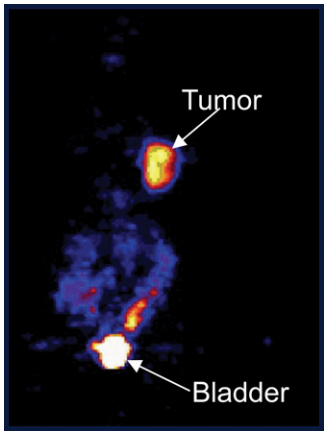

FIGURE 2. Preclinical ^{18}F-DEG-VS-NT PET for neurotensin receptor-1 targeted imaging. High targeting in tumor with low renal uptake was seen at 2 hours after injection.

Another example came from Guo et al. from the Massachusetts General Hospital and the Martinos Center for Biomedical Imaging (Boston, MA), who reported on "PEG-like multimodal nanoprobes as imaging agents" [271]. Their agent has the ability to deliver early-phase blood pool images in brain angiography with 2-photon fluorescent microscopy as well as delayed-phase SPECT/CT imaging without hepatic uptake (Fig. 5). These results are preclinical but indicate the potential for in-human applications of tracers with more than one functionality and more than one molecular imaging modality.

Hong et al. from the University of Wisconsin (Madison) and TRACON Pharmaceuticals (San Diego, CA) reported on "Red fluorescent ZnO nanoparticle as a novel platform for cancer targeting and imaging" [439]. Zinc has an intrinsic red fluorescence, which makes it attractive for optical as well as radionuclide imaging.

One of our current challenges is in addressing the epidemic of esophageal carcinoma. Premalignant lesions can occur in the form of Barrett esophagus, often associated with reflux. Yet these lesions can be difficult to identify on endoscopy. Habibollahi et al. from the Massachusetts General Hospital (Boston, MA) and the Hospital of the University of Pennsylvania (Philadelphia) reported on "Optical molecular imaging of periostin, a biomarker for tumor invasiveness" [273]. The authors looked for early changes in periostin levels that could be associated with esophageal dysplasia. With near-infrared spectroscopy and a periostin-targeting agent they were able to secure a high signal in severe dysplasia (Fig. 6). The translation pathway for this kind of approach is not as daunting as in some other areas, because optical imaging is quite feasible in the esophagus,

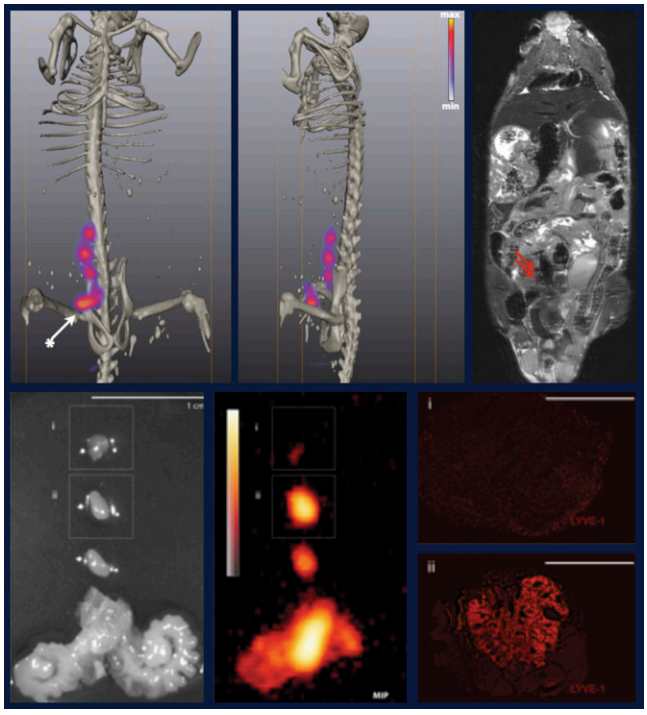

FIGURE 4. ^{89}Zr-ferumoxytol iron oxide nanoparticles for multimodality PET/MR lymph node mapping. Preclinical example of deep-tissue lymph node mapping drainage from the prostate after injection of ~5 μL of tracer into the right anterior prostate. PET/CT (left) shows the injection site (arrow) and a chain of draining lymph nodes. These can be seen on MR (right), and signal from these tissues can also be used in the surgical setting (using radioguided probes or Cerenkov imaging) to guide resection of tissues and to confirm resection. The prostate (bottom) and 3 resected tissues are shown. Ex vivo micro-PET shows that one of the suspected nodes is connective tissue, as confirmed by staining for lymphatic endothelium (bottom right).

where the target is in close proximity to incident light and the detection instrument.

New PET tracers are continually being investigated in human studies, and new tracers continue to enter clinical use. Davidzon et al. from Stanford University Medical Center (CA) reported on "Biodistribution and kinetics of the novel PET/CT radiopharmaceutical ^{18}F-FPPRGD2 in cancer patients" [11]. The tracer is based on the drug cilengitide, an integrin-binding cyclic RGD pentapeptide. Figure 7 shows good targeting in 3 foci in a patient with newly diagnosed breast cancer. It is noteworthy that these results were seen in an ^{18}F-FDG–negative lobular carcinoma.

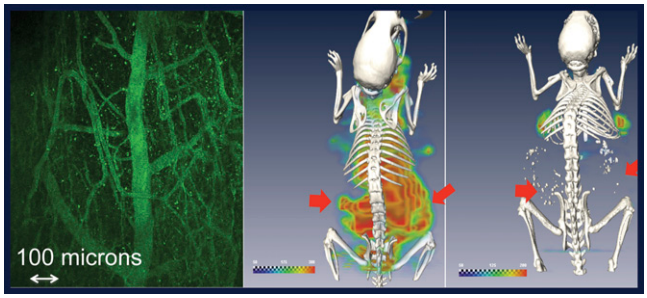

FIGURE 5. PEG-like multimodal nanoprobes as imaging agents in brain angiography, paired with long-circulating fluorescein in 2-photon microscopy (left) and in SPECT/CT of tumor (arrows) enhanced permeability and retention effect with a long-circulating $^{111}In^{3+}$ without hepatic uptake (right, at 2 and 48 hours after injection).

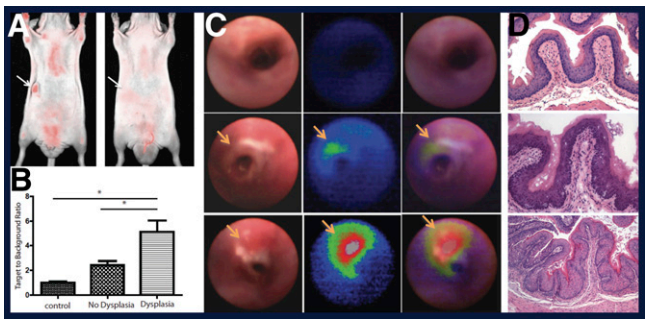

FIGURE 6. Optical molecular imaging of periostin. Left: Fluorescent images of periostin optical probe in tumor xenografts of TE-11 (periostin+) and TT (periostin–) showing high uptake in positive tumors. Middle block: Representative dual-channel endoscopy images from a normal mouse (top row) and mice with single (no dysplasia, middle row) and double knockout p120 gene (bottom row, severe dysplasia). Intense fluorescence signal is seen in the mouse with double knockout of the p120 gene, which results in severe dysplasia and high expression of periostin. Right block: H&E staining of esophageal tissue showing normal tissue, slight hyperplasia but no dysplasia, and severe dysplasia in esophagus.

Imaging Devices

Our tools for evaluating molecular imaging devices depend on extensive development and good imaging studies in animals. Tsui et al. from Johns Hopkins University (Baltimore, MD), TriFoil Imaging (Northridge, CA), and Gamma Medica Inc. (Northridge, CA) reported on "A completed SPECT/MR insert for simultaneous SPECT/MR imaging of small animals" [595]. This device allows for simultaneous SPECT and MR imaging with relatively rapid image production. Figure 8 shows various investigational images and demonstrates the feasibility of moving to SPECT/MR in animals and, eventually, in humans.

One of the challenges of increasingly sensitive molecular breast imaging is the question of what to do when lesions are identified. Radionuclide-guided breast biopsies are essential, because the lesions cannot always be identified on ultrasound.

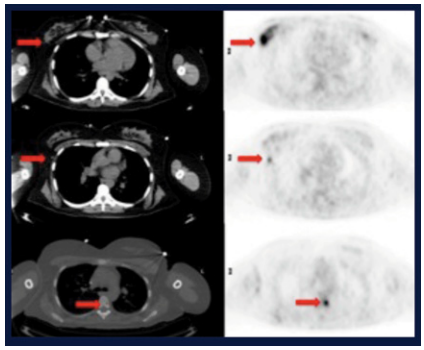

FIGURE 7. ^{18}F FPPRGD$_2$ PET/CT in 44-year-old premenopausal woman with a newly diagnosed $T_3N_2M_1$ multicentric lobular carcinoma of the right breast shows the primary right breast lesion, right axillary lymph node, and thoracic spine metastases (all biopsy-proven). ^{18}F FDG PET/CT (not shown) did not identify these lesions.

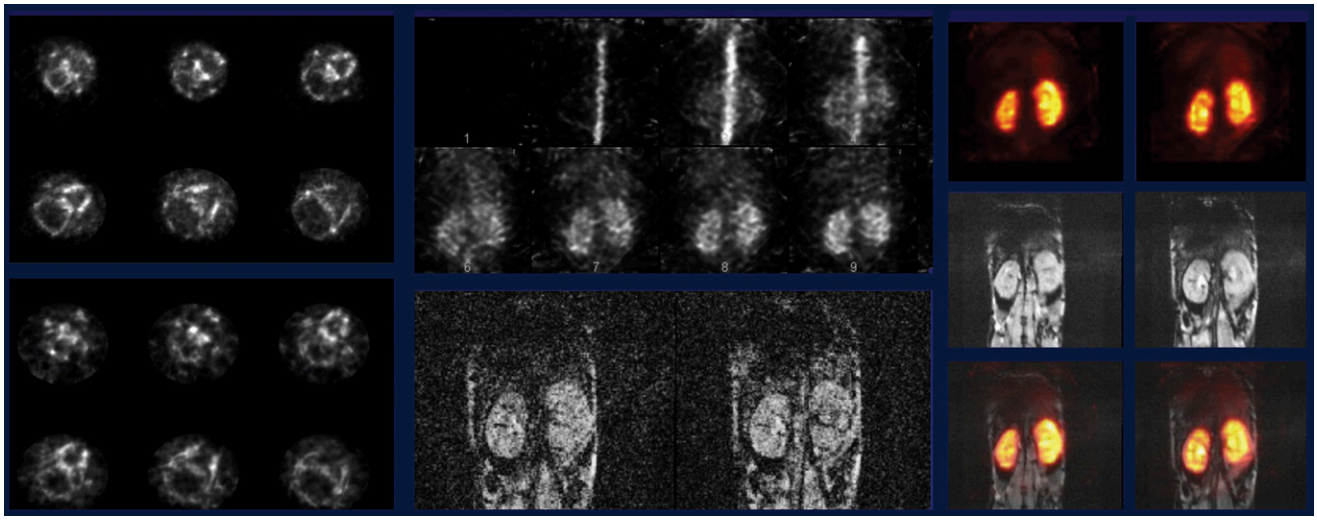

FIGURE 8. Investigational images acquired with a SPECT/MR insert for simultaneous SPECT/MR imaging of small animals. Left: ^{99m}Tc-MDP acquisitions at 18- and 36-pinhole resolution in a mouse head with stand-alone SPECT acquisition. Middle: ^{99m}Tc-MAG3 renal imaging in a mouse with 10 seconds/frame dynamic SPECT (top) and 80 seconds/frame dynamic MR. Right: ^{99m}Tc-MAG3 renal imaging in a mouse, including 30-minute summed SPECT (top), 30-minute summed MR (middle), and 30-minute fused SPECT/MR image.

Hugg et al. from Gamma Medica, Inc. (Northridge, CA) and BLN Scientific (Bethesda, MD) reported on "Biopsy guided by molecular breast imaging" [482]. The authors added a cadmium-zinc-telluride (CZT) gamma camera to their 2-camera approach. This additional camera was able to guide placement of the biopsy needle into the lesion, with promise for allowing visualization, localization, biopsy guidance, and verification of targeting on sample imaging.

In addition to localization devices for lesions in the breast, an effort is underway to develop devices for localization of prostate cancer. Franc et al. from Radiological Associates of Sacramento (CA), Johns Hopkins University (Baltimore, MD), Brookhaven National Laboratory (Upton, NY), Diagnostic Pathology Medical Group (Sacramento, CA), and the University of California San Francisco (CA) reported on "Transrectal gamma imaging of the prostate: potential for localization of cancer" [1588]. The device is designed to be placed into the rectum and in close proximity to the prostate, facilitating prostate imaging. We still need a good prostate imaging agent to pair with this, but the potential availability of an endorectal prostate imaging device is promising. In their exploratory study, these authors decribed safety and first-in-human imaging experience with transrectal gamma imaging with the endoluminal CZT-based compact camera after administration of ^{111}In-capromab pendetide in patients with biopsy-proven, untreated primary prostate cancer as well as those without prostate cancer

The potential for PET/MR imaging in the brain and in the heart is clear, and researchers at the SNMMI meeting reported on investigations to improve and expand this hybrid imaging approach. Levin et al. from Stanford University School of Medicine (CA) and GE Healthcare (Waukesha, WI) reported on "Prototype time-of-flight PET ring integrated with a 3T MR imaging system for simultaneous whole-body PET/MR imaging" [148]. Their insert uses silicon photomultiplier photodetectors, with the potential for better time-of-flight information than existing approaches. Images with this insert are quite impressive. Figure 9 shows no substantial degradation of PET image quality with simultaneous PET/MR acquisition. These efforts to improve the quality of PET/MR imaging constitute attractive progress in our field.

What about the utility of PET/MR? Al-Nabhani et al. from University College London (UK) reported on the "Potential clinical utility of PET/MR imaging in oncological patients" [234]. Using the Philips PET/MR apparatus, this group found good correlation between whole-body PET/MR and PET/CT imaging results. PET/MR changed management in 6.5% of patients, mostly in the pelvis, where the soft tissue contrast of MR imaging delineated pathology. Figure 10 shows imaging in a patient in whom a residual paraganglioma was suspected after resection, with 2 foci seen on PET/MR that were not seen on PET/CT. This was part of a larger study in which a total of 189 ^{18}F-FDG–avid foci were identified on both PET/CT and PET/MR imaging. On evaluation of PET/CT studies, 32 of these foci were believed to be physiologic or nonpathologic uptake because of lack of corresponding CT abnormality. On PET/MR imaging, 11 of these 32 lesions were found to correspond to sites of disease as indicated by the presence of soft tissue or altered signal intensity. The authors noted overall improvement with PET/MR in their confidence in assessing anatomic extent of disease in 6.5% (7.9% in soft tissue/nerve infiltration at primary site and 12% at metastatic sites) of studies.

MR can be encoded to display motion and potentially used to incorporate MR positioning information into PET, so that gating can be achieved with dynamic MR acquisition as opposed to CT, thus sparing radiation. An early example of this was presented by Petibon et al. from Massachusetts General Hospital and the Harvard Medical School (Boston, MA), who reported on "MR-based motion correction in simultaneous PET-MR liver imaging" [68].

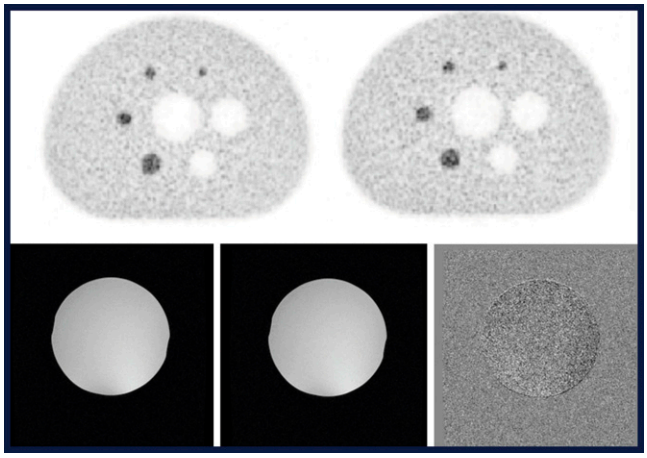

FIGURE 9. Prototype time-of-flight PET ring integrated with 3T MR imaging for simultaneous whole-body PET/MR imaging. Top: No substantial degradation of PET image quality (left, PET with MR idle) was seen with simultaneous PET/MR acquisition (right) in a National Electrical Manufacturers Association image quality phantom. Bottom: No substantial degradation of MR image signal-to-noise ratio (left, with PET off) was seen with simultaneous PET/MR acquisition (middle). Subtraction image is at right.

Issues with quantitation and attenuation correction (AC) are challenging in PET/MR, because we do not measure directly by CT AC and, at least so far, most PET/MR AC algorithms have been mixtures of data from varying MR sequences. In a couple of papers at this meeting, time-of-flight data from emission datasets in PET were used to generate an attenuation map for use in PET/MR and to refine further the attenuation maps made from MR. One of these papers came from Boellaard et al. from the VU University Medical Center (Amsterdam, The Netherlands), who reported on "Accurate whole-body PET/MR quantification using time-of-flight and maximum likelihood of reconstruction of attenuation and activity" [151].

Quantitation

Quantitation has always been an important element in our field but has moved from a goal in principle to a significant requirement in practice. To achieve the kinds of quantitation that will move the field forward, we need standardization, refined approaches to image analysis, and a clearer definition of what should be analyzed qualitatively and what quantitatively. Tumors have many parameters, including but not limited to volume, standardized uptake value (SUV), total lesion glycolysis, and hetereogeneity. If we are going to incorporate measures of these elements into daily practice, then we will need to simplify quantitative techniques and, where possible, automate them.

Scheuermann et al. from the University of Washington (Seattle), the American College of Radiology Imaging Network (Philadelphia, PA), and the University of Pennsylvania (Philadelphia) reported on "Qualification of National Cancer Institute (NCI)–designated Comprehensive Cancer Centers for quantitative PET/CT imaging in clinical trials" [334]. More than 60 of the NCI Cancer Centers are participating in an NCI-initiated program to create a network of "trial-ready" Centers of Quantitative Imaging Excellence (CQIE). In this program, 64 out of 65 scanners qualified for CQIE inclusion, but $<40\%$ of these were qualified on their first submission. The program criteria include uniformity, contrast, and clinical quality. Initial data suggest that qualification by a centralized core lab may be important to ensure quantitatively accurate trial data across multiple sites (Fig. 11).

PET has been in clinical use for a sufficient period that it might be assumed that we would be in general agreement on ^{18}F-FDG dose for PET examinations. Del Sole et al. from the University of Milan (Italy) reported on "An international multicenter comparison of ^{18}F-FDG injection protocols and radioactive dose administered to patients undergoing ^{18}F-FDG PET examinations" [372]. These authors compared doses administered and found that U.S. doses on average were 46.7% larger than those in Italy. This clearly demonstrates an opportunity for global standardization of doses, with the potential for dose reduction.

To perform PET studies to assess treatment response, it is important to know the extent to which our methodologies are reproducible. Because metabolic tumor volume is increasingly seen as part of the method for identifying total tumor burden in patients, information on the repeatability of metabolic tumor volume is significant and informative. Frings et al. from the VU University Medical Center (Amsterdam, The Netherlands) and Bristol-Myers Squibb (Princeton, NJ)

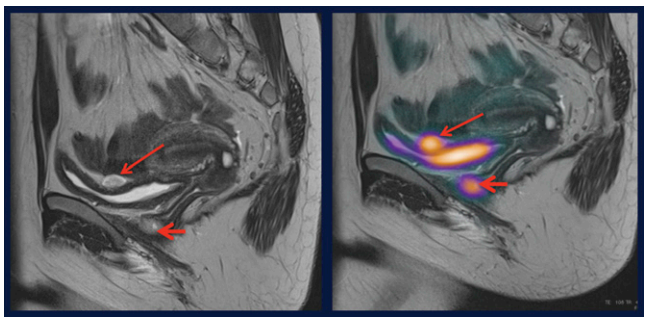

FIGURE 10. Images acquired in a 16-year-old girl with suspected recurrence after resection of paraganglioma. (A) Sagittal T2WI MR. (B) Sagittal ^{68}Ga-DOTATATE PET and T2WI MR fused. The 2 foci (arrows) were not seen on the original PET/CT.

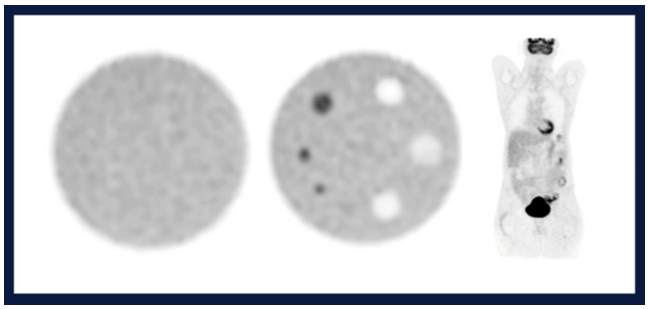

FIGURE 11. The National Cancer Institute's Centers of Quantitative Imaging Excellence Program qualifies PET scanners on uniformity (left), contrast (middle), and clinical quality (right).

reported on "Repeatability of metabolically active tumor volume of ^{18}F-FDG PET-CT in a multicenter setting" [14]. They assessed 19 different methodologies for analyzing tumor volume, with results indicating substantial variability among results with these methods. They found those methods based on SUV_{max} to be the most variable, with those based on contrast-oriented 50% of SUV_{peak} to be the most reliably repeatable. The way in which we measure matters, and as we evolve toward quantitative PET imaging we will have to move to methods on which we can depend for consistency from study to study.

Heterogeneity was discussed in a number of papers at the SNMMI 2013 meeting. Recent oncologic studies indicate that cancers are not the same throughout the body. Clonal evolution occurs, and clones that are the most aggressive are most likely to kill patients, whereas other clones may not contribute significantly to mortality. Heterogeneous tumors, then, can logically be considered to be linked to poorer prognoses. Son et al. from Kyungpook National University Hospital (Daegu, Korea) reported on "Prognostic implication of intratumoral metabolic heterogeneity in invasive ductal breast cancer patients" [1442]. Their analyses showed that overall survival was higher with more uniform (less heterogeneous) tumors. Cook et al. from Kings College London (UK) and Royal Marsden Hospital (London, UK) reported on "Textural analysis of ^{18}F-FDG PET to assess response to erlotinib in non–small cell lung cancer (NSCLC)" [566]. They found that baseline heterogeneity and changes in heterogeneity are predictive and prognostic in this patient group. Vailla et al. from CHU Poitiers (France) and INSERM UMR (Brest, France) reported on "Qualitative versus quantitative assessment of intratumoral FDG heterogeneity for assessing patient outcome in NSCLC" [1587]. These groups of authors have measured heterogeneity in a variety of ways, but, in general, reports at this meeting showed that the more heterogeneous tumors tend to be the most challenging. We may need to move toward more multiparametric descriptors for tumors to fully appreciate and incorporate the relevance of heterogeneity into clinical practice.

Goulon et al. from University Hospital Nantes, the Institut de Cancérologie de l'Ouest Nantes, and INSERM (all in Nantes, France) reported on "Comparison of different indices for metabolic PET assessment according to PET Response in Solid Tumor (PERCIST) in metastatic breast cancer" [1416]. This retrospective study compared the performance of metabolic assessment, according to PERCIST criteria, using 6 different indices in metastatic breast cancer patients treated with chemotherapy or hormone therapy. Their results suggested that SUV_{max}, SUV_{peak}, and SUV_{mean} appeared to be better in assessing therapy response than standardized added metabolic activity, metabolic volume, or total lesion glycolysis. This literature is emerging, and it is important to know that a variety of criteria are being used to make these assessments of treatment response.

O et al. from Johns Hopkins University (Baltimore, MD) received a Young Investigator Award at this meeting for reporting that a "Change in tumor-to-liver uptake ratios is comparable to PERCIST 1.0 in predicting complete response in primary breast cancer systemic therapy" [123]. This work showed that a very simple approach, looking at changes in tumor/liver uptake, was comparable to percentage change in peak standardized uptake normalized to lean body mass (SUL_{peak}) in predicting complete response in neoadjuvant breast cancer chemotherapy. This type of relative (as opposed to "absolute") quantitation can be quite helpful in analyses and is simple and easy to perform.

Dr. O and colleagues from Johns Hopkins University (Baltimore, MD) and the Dana Farber Cancer Institute (Boston, MA) also asked ""How many lesions to measure for response assessment: comparing SUL_{peak} changes in single lesion and the sum of the 5 hottest lesions in 3 types of cancer and 3 types of therapy" [229]. The group looked at 3 kinds of tumors: sarcoma, treated with insulin-like growth factor-1 receptor antibody; lymphoma, treated with Bexxar; and breast cancer, treated with carboplatin and paclitaxel with or without vorinostat. They found that the percentage change in the single hottest tumor SUL_{peak} was equivalent to or slightly more informative than change in the sum of up to 5 of the hottest tumor SUL_{peaks}.

Some researchers ask whether quantitation is always necessary. Györke et al. from ScanoMed Medical Diagnostic Research and Training Ltd. (Budapest, Hungary) and an international consortium of medical centers reported on "The prognostic role of interim FDG PET in diffuse large B-cell lymphoma performed after 2 cycles of chemoimmunotherapy: comparison of visual and semiquantitative evaluation" [1569]. In this International Atomic Energy Agency–coordinated study, as expected, unequivocally negative PET was associated with good clinical results and unequivocally positive PET was associated with less favorable clinical outcomes. But we may be simplistic in trying to categorize PET results in these settings as either positive or negative. Their results demonstrated a middle range of equivocal PET in which prognosis was intermediate between good and poor outcomes. We should remember that the biology we study and the resulting imaging data are intrinsically continuous and that forcing ourselves to dichotomize data when it is not really dichotomous in terms of outcomes is probably not optimal.

SPECT is becoming more quantitative. With AC as a part of SPECT/CT, we have the possibility of more easily attainable SPECT quantitation. Zhu et al. from the Peking Union Medical College Hospital (Beijing, China), a consortium of Chinese hospitals and academic centers, and GE Healthcare (Beijing, China) reported on "SPECT response criteria in solid tumors (SPERCIST) based on integrin receptor imaging: compared with Response Evaluation Criteria in Solid Tumors (RECIST) and PERCIST" [1582]. Their results suggest that their SPERCIST criteria have predictive capabilities superior to those of RECIST.

Measurement is important in conventional radiology, and new questions arise in the context of hybrid imaging.

One such question is whether we need contrast CT in measurement of lymphoma. Sosa et al. from the Mount Sinai Medical Center (New York, NY) reported that "Lymph node measurements based on low-dose FDG-PET/CT appear equivalent to those obtained by contrast-enhanced CT in lymphoma" [1565]. The researchers found that not only were the 2 approaches equivalent in results but that contrast CT as part of PET/CT contributed little or no additional information in terms of tumor size (Fig. 12). These data suggest that radiation burden could be reduced by using noncontrast CT imaging in PET/CT.

Putting quantitation into practice in the clinical setting is challenging. Okizaki et al. from Asahikawa Medical University Hospital (Japan) reported on "A utilization of SUV navigator interface to reduce the time on film reading of ^{18}F-FDG PET/CT" [1629]. The authors' software tool contributed to up to 50% reductions in time required to read PET/CT images when several lesions were present. These types of expert tools are important in integration of quantitation into daily practice.

Preclinical and Clinical Biology

Several papers at the meeting focused on the interface between preclinical and clinical biology. Heidari et al. from the Massachusetts General Hospital and the Dana Farber Cancer Institute (Boston, MA) reported on "Monitoring the effect of 5'-adenosine monophosphate-activated protein kinase (AMPK) activators and fatty acid synthase inhibitors in prostate cancer with ^{11}C-acetate PET" [507]. Their results showed that the time of last therapy may affect acetate imaging. In fact, ^{11}C-acetate may not be a good marker for monitoring response to therapy with indirect inhibitors of fatty acid synthase such as AMPK activators in prostate cancer.

Stems cells and regenerative biology are an increasing focus in oncologic studies. Kim et al. from Seoul National University College of Medicine (Republic of Korea) reported on "Development of codon-optimized sodium/iodide symporter for a sensitive imaging reporter gene and an efficient therapeutic gene" [65]. These researchers showed significant increases in uptake in vivo in vectors of stem cells with an optimized symporter cassette installed, in comparison with the conventional cassette (Fig. 13). This is a promising tool for cancer biology.

Rates of head and neck cancer are also increasing, especially the human papilloma virus (HPV)–associated types, as reflected in studies at this meeting. Tahari et al. from Johns Hopkins University (Baltimore, MD) reported on "FDG PET/CT imaging of oropharyngeal squamous cell carcinoma: characteristics of HPV-positive and HPV-negative tumors" [457]. The authors found that HPV-negative tumors had a higher SUV_{max} and were larger than HPV-positive tumors. However, lymph node metastases in HPV-positive patients were larger and had higher tumor lesion glycolysis than those in HPV-negative patients. This difference between primary tumor and metastases in head and neck cancer, especially HPV-associated disease, may be important to keep in mind when interpreting imaging studies.

Cancer Diagnosis, Phenotyping, Multimodal, Staging

Many presentations at the SNMMI 2013 meeting focused on aspects of diagnosis, staging, restaging, assessing prognosis, assessing treatment response, and surveillance. Löfgren et al. from the Rigshospitalet (Copenhagen, Denmark) and cmi-experts GmbH (Zürich, Switzerland) reported on "Diagnosing bone metastases: pilot data from a prospective study comparing ^{99m}Tc-methyl diphosphonate planar bone scintigraphy, whole body SPECT/CT, ^{18}F-fluoride PET/CT and ^{18}F-fluoride PET/MRI" [93]. In this study in patients with prostate cancer, the researchers found that ^{18}F-fluoride PET/CT was consistently better than planar or SPECT/CT imaging.

Because PET has now been widely available for some time, we have more data available on rarely occurring cancers. Hu et al. from Fudan University (Shanghai, China) reported on "^{18}F-FDG PET/CT in the evaluation of testicular nonseminomatous germ cell cancer after orchiectomy and chemotherapy" [290]. Based on results in 40 patients, the sensitivity, specificity, and accuracy of ^{18}F-FDG PET/CT for evaluation of residual tumor viability were 94.1% (16/17), 87.0% (20/23), and 90.0% (36/40), respectively. The practical implication is that patients with this rare tumor who are successfully treated can be followed without the need for surgery to explore the nodes.

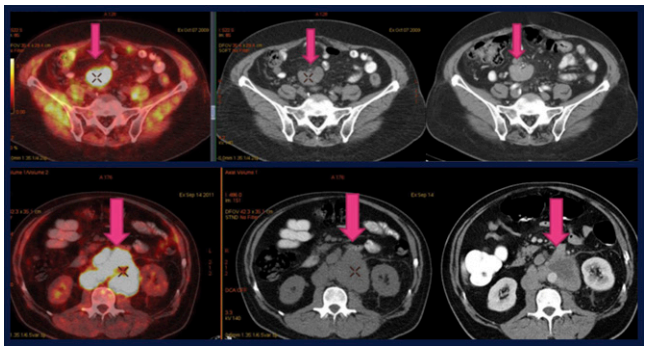

FIGURE 12. Lymph node assessment based on low-dose PET/CT. The researchers found that contrast CT as part of PET/CT contributed little or no additional information in terms of tumor size.

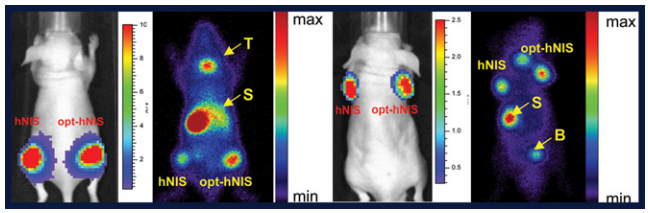

FIGURE 13. Codon-optimized sodium/iodide symporter for a sensitive imaging reporter gene and an efficient therapeutic gene. Left 2 images: In a xenografted breast cancer cell line (MDA-MB231) bioluminescent (left) and gamma camera images showed the difference between humanized and codon-optimized sodium-iodide symporters. Right 2 images: Corresponding images acquired in a xenografted thyroid cancer cell line. Uptake in the codon-optimized xenografts was significantly higher.

Lymphatic Imaging. We are familiar with lymph node imaging with ^{18}F-FDG PET, but less data are available on ^{18}F-fluorothymidine (^{18}F-FLT) PET. Nakajo et al. from Kagoshima University Graduate School of Medical and Dental Sciences (Japan) and Nanpuh Hospital (Kagoshima, Japan) reported on the "Effect of pathological factors on visibility of lymph node metastasis from colorectal cancer with FLT PET/CT" [637]. A total of 536 regional lymph nodes were dissected in 28 patients. The majority were pathologically negative, but metastasis was microscopically noted in 37 regional lymph nodes of 13 patients, indicating a sensitivity and specificity of 32% and 98.8%, respectively, for ^{18}F-FLT PET/CT. PET-positive nodes were larger and had a higher proliferative fraction and a higher thymidine kinase-1 level than PET-negative nodes. This suggests that although ^{18}F-FLT PET/CT is highly specific, it will fail to detect the majority of tumor-involved nodes.

In the last few months, ^{99m}Tc-tilmanocept was approved by the U.S. Food and Drug Administration (FDA). Baker et al. from the University of California, San Diego (La Jolla) reported that "^{99m}Tc-tilmanocept (Lymphoseek) identifies more positive nodes using fewer SLNs compared to ^{99m}Tc-sulfur colloid in early-stage breast cancer patients" [016]. They found that although ^{99m}Tc-tilmanocept localized in fewer SLNs, it was able to detect a significantly greater percent of tumor-positive SLNs in the node-positive population. This suggests a higher diagnostic yield and fewer false-positive nodes with this tracer. The same group, under Liss, reported on "SLN mapping via fluorescence imaging of a multimodal receptor-binding probe" [275]. They described robotic-assisted SLN mapping for both ^{68}Ga PET and optical imaging (Fig. 14).

Van den Berg et al. from Leiden University Medical Center (The Netherlands) and the Antoni van Leeuwenhoek Hospital (Amsterdam, The Netherlands) reported on "Combined radio- and fluorescence-guided sentinel node biopsy in a large cohort of melanoma patients" [667]. They showed multimodal imaging in humans using indocyanine green for optical sentinel node identification. The fluorescence component allowed identification of sentinel nodes even when these nodes failed to accumulate blue dye (Fig. 15).

Prostate Cancer. As we know, ^{18}F-FDG has some limitations in prostate cancer, except in the setting of disseminated disease. Zacho et al. from Viborg Hospital (Denmark) and a consortium of other hospitals in Denmark reported on a "Prospective multicenter study of bone scintigraphy in consecutive patients with newly diagnosed prostate cancer" [288]. The study included 635 patients, and the authors found that no patients with a prostate-specific antigen (PSA) level $<$10 ng/mL had bone metastases, irrespective of other findings. Metastases were rare even in patients with PSA $<$20 ng/mL, except in those cases in which the tumor was aggressive. This suggests bone scanning for patients with low PSAs may be inappropriate.

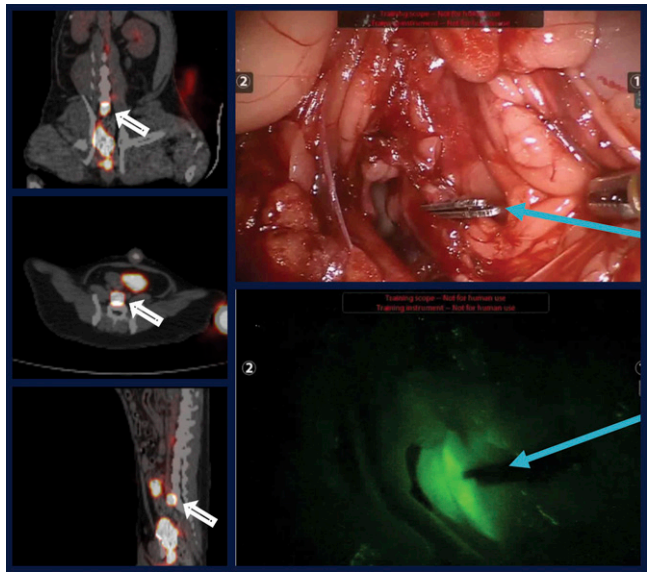

FIGURE 14. Robotic-assisted sentinel lymph node (SLN) mapping with ^{68}Ga- and ^{99m}Tc-infrared dye 800 CW-tilmanocept. Left column: PET/CT cross-sections at 1 hour after injection in coronal (top), transaxial (middle), and sagittal (bottom) views. Arrows point to presacral SLN. Right column: Robotic-assisted SLN mapping 36 hours after injection in brightfield view (top) and fluorescence view (bottom). Arrows point to surgical clip.

Brendle et al. from University Hospital Tübingen (Germany) reported on "PET/CT and simultaneous MR/PET in patients with suspicion of prostate cancer recurrence: diffusion-weighted imaging and ^{11}C-choline uptake for N staging" [342]. The researchers found that delayed ^{11}C-choline imaging appeared to better distinguish between benign and malignant lymph nodes than did early choline images. The apparent diffusion coefficient was found to be lower in malignant than in benign lesions. It is possible that by combining PET and MR quantitative parameters that better phenotyping of nodes will be feasible than is possible by either PET or apparent diffusion coefficient analyses alone.

Eiber et al. from the Technische Universität München (Germany) reported on "Initial experience in restaging of patients with recurrent prostate cancer: comparison of ^{11}C-choline PET/MR and ^{11}C-choline PET/CT" [343]. In their example images, PET showed a very faint uptake of choline in the former prostate fossa with no additional information provided by CT (Fig. 16). In subsequent PET from PET/MR a faint area of focal uptake was seen in the same position. High-resolution T2-weighted MR images showed that this uptake was not retained urine in the urethra but located in the soft tissue. The addition of dynamic contrasted-enhanced MR image showed an arterial hypervascularized lesion in the same region consistent with tumor. PET/MR imaging is particularly promising in this setting.

Cho et al. from Johns Hopkins University (Baltimore, MD) reported on "Preliminary evaluation of ^{18}F-DCFBC prostate-specific membrane antigen (PSMA) PET for detection of primary prostate cancer" [286]. This group has previously

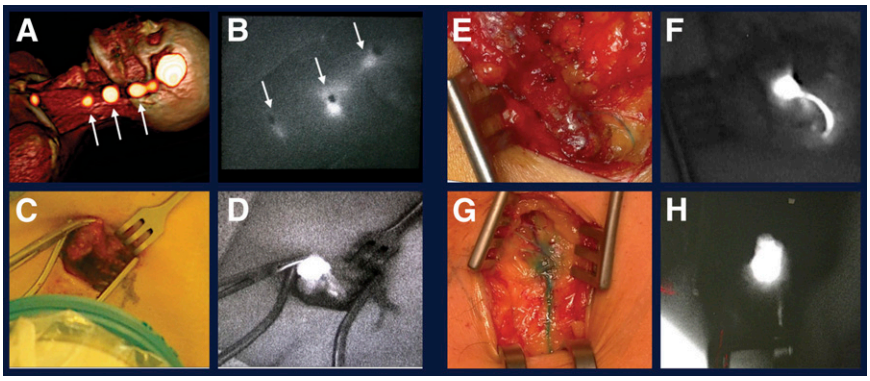

FIGURE 15. Optical sentinel node (SN) identification. The fluorescence component of this approach allows identification of sentinel nodes even when they fail to accumulate blue dye. Occasionally, when SNs are located superficially, SNs can be seen through the skin (A,B). Remaining images show detection of an SN when no blue dye was used (C,D), when only a blue vessel was found running to the SN (E,F) or when the lymphatic vessel and SN were stained blue (G,H).

shown that lesions in metastatic prostate disease can be identified with this low-molecular-weight peptide that binds to PSMA. They showed several examples at this meeting in which the PET agent could identify the primary tumor when PET and MR were fused with software (Figs. 17, 18). This is promising work on in situ imaging of prostate cancer.

Taleghani et al. from Emory University (Atlanta, GA) reported on "Utility of anti-3-[^{18}F] FACBC PET/CT to predict early biochemical failure following salvage cryotherapy for recurrent prostate cancer" [345]. Figure 19 shows images from patients after cryotherapy, in which higher SUV_{max} was seen to correlate with early treatment failure. Emerging data with this agent are encouraging.

Kwee et al. from the Queen's Medical Center (Honolulu, HI) reported on "Whole-body tumor burden measured on ^{18}F-fluorocholine PET/CT and survival in metastatic castrate-resistant prostate cancer (CRPC)" [1600]. The researchers noted that fluorocholine uptake correlated with survival and concluded that quantitative tumor burden estimates from ^{18}F-fluorocholine PET/CT may provide independent prognostic information in metastatic CRPC.

Nanni et al. from the S. Orsola-Malpighi Hospital (Bologna, Italy) reported on "^{18}F-FACBC vs ^{11}C-choline PET/CT in patients with radically treated prostate cancer and biochemical relapse: preliminary results" [1601]. They showed several examples in which ^{11}C-choline PET/CT was negative but ^{18}F-FACBC was positive in lymph nodes and bone metastases, making the latter a promising tracer for prostate cancer detection (Fig. 20).

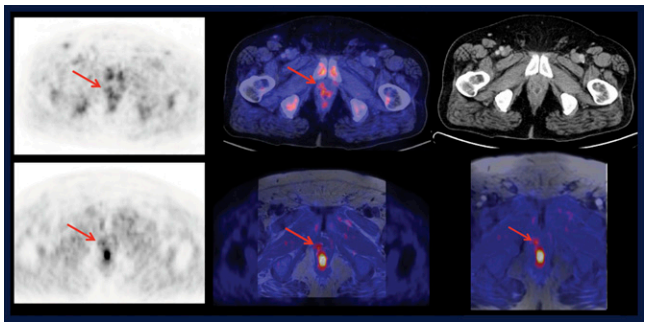

FIGURE 16. Comparison of PET/CT and PET/MR in local recurrence of prostate cancer. Top row: PET alone from PET/CT shows a very faint uptake of choline in the former prostate fossa with no additional information provided by fusion (middle) with contrast-enhanced CT (right). Bottom row: In the subsequent PET from PET/MR a faint uptake was seen in the same position. Fusion (middle) with high-resolution T2-weighted images showed that this uptake was not retained urine in the urethra but was located in the soft tissue. The addition of dynamic contrasted-enhanced MR imaging (right) showed an arterial hypervascularized lesion in the same region.

Treatment Monitoring and Posttreatment Assessment

Lau et al. from the Austin Hospital (Melbourne, Australia) and University of Melbourne reported on "^{18}F-FDG PET for colorectal liver metastases: metabolic response to preoperative chemotherapy predicts prognosis" [640]. They showed that patients with a better metabolic response on PET/CT showed better 3-year survival than those who were unresponsive, in both metastatic and primary disease. In this study the RECIST criteria were found to have little prognostic value.

Nielsen et al. from the VU University Medical Center (Amsterdam, The Netherlands) reported on "PET-CT after radiofrequency ablation of colorectal liver metastases: suggestions for timing and image interpretation" [67]. In a study of

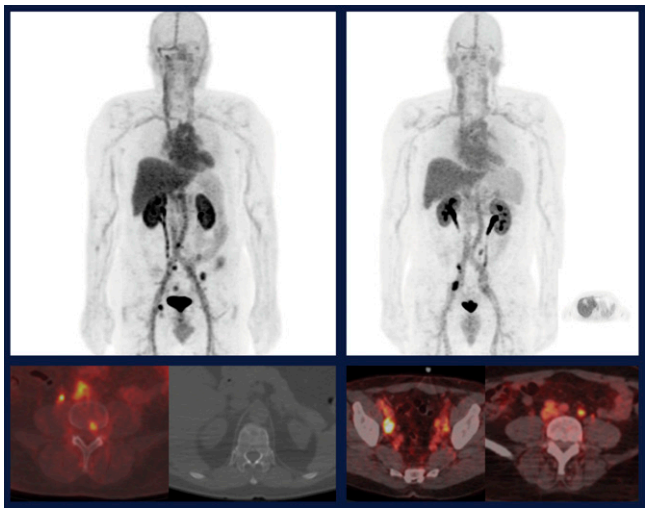

FIGURE 17. ^{18}F-DCFBC low-molecular-weight prostate-specific membrane antigen PET imaging in detection of metastatic and primary prostate cancer. Left: in a patient with bone metastases. Right: In a patient with lymph node metastases. Results with this agent correlated with PET/CT imaging results (bottom rows).

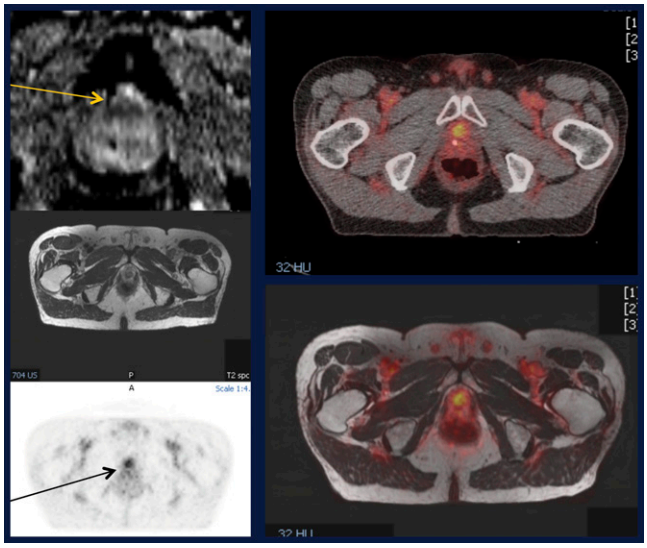

FIGURE 18. ^{18}F-DCFBC low-molecular-weight prostate-specific membrane antigen PET imaging in detection of prostate adenocarcinoma. Left column: 3T diffusion-weighted MR image (top), T2-weighted MR image (middle), and 2D PET pelvic image (bottom) showing focal abnormal PET uptake right of midline apex of prostate. Right column: fused PET/CT (top) and software-fused PET/MR image (bottom).

79 patients, focal uptake was found to be highly suggestive of local site recurrence. They also noted that rim-shaped uptake caused by inflammation can complicate image interpretation up to 5 months after radiofrequency ablation (Fig. 21).

O et al. from Johns Hopkins University (Baltimore, MD) and the University of Michigan (Ann Arbor, MI) reported that "Early treatment response by FDG PET in patients with the Ewing sarcoma family of tumors from the SARC-11 trial predicts survival" [600]. In a large group of patients assessed by visual response, European Organisation for Research and Treatment of Cancer criteria, and PERCIST criteria, it was possible to characterize patients as responders or nonresponders with a high degree of accuracy

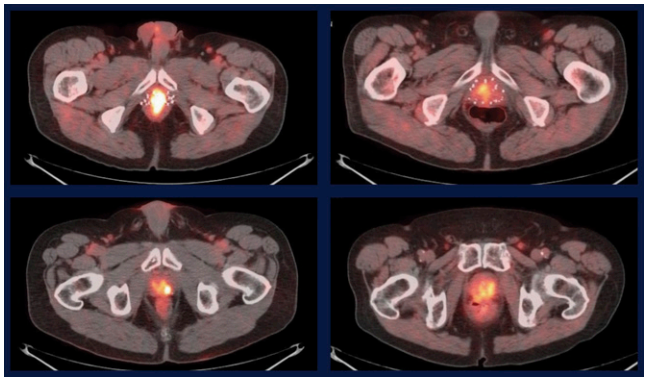

FIGURE 19. Representative anti-3-^{18}F-FACBC PET/CT images in patients with similar prostate-specific antigen (PSA) levels but different SUV_{max} at 17 minutes. Top row: patients with low PSAs of 2.2 (left, with an SUV_{max} of 6.5 and early failure) and 1.6 (right, with an SUV_{max} of 2.2 and no early failure). Bottom row: patients with high PSAs of 9.3 (left, with an SUV_{max} of 10.9 and early failure) and 10.4 (right, with an SUV_{max} of 4.4 and no early failure).

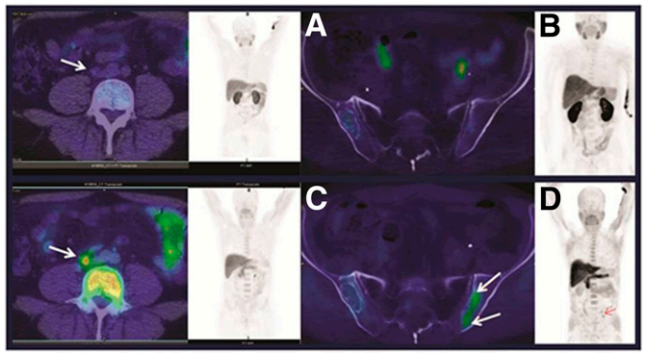

FIGURE 20. ^{18}F-FACBC and ^{11}C-choline PET/CT in patients with radically treated prostate cancer and biochemical relapse. Left block: images acquired with ^{11}C-choline (top) and ^{18}F-FACBC (bottom). The right common iliac lymph node (arrows) was negative on choline imaging but positive with ^{18}F-FACBC. Right block: images acquired with ^{11}C-choline (top) and ^{18}F-FACBC (bottom). The left sacroiliac joint (arrows) was negative on choline imaging but positive with ^{18}F-FACBC.

after only 9 days of therapy. Overall survival at 300 days could be predicted in these patients by an early ^{18}F-FDG PET scan at just 9 days.

Lovinfosse et al. from CHU de Liège and the Université de Liège (Belgium) reported on "Prognostic value of FDG PET/CT in patients with lung tumors treated by Cyberknife" [567]. The most predictive data in this study turned out to be baseline data rather than posttreatment data. RECIST response was not correlated with any metabolic parameters nor with overall survival, but baseline SUV_{max} on PET predicted overall survival.

Hartenbach et al. from Ludwig-Maximilians-University Munich (Germany), the German Armed Forces Institute of Radiobiology, the German Armed Forces Hospital (Ulm), and the German Federal Ministry of Defence reported on "Molecular imaging after external irradiation: a multiparametric approach for the assessment of radiation effects" [332]. The authors evaluated the potential of PET imaging with ^{68}Ga-NODA-GA-annexin V (to assess cell death) and ^{18}F-FLT (to assess proliferation) for evaluation of dose-dependent effects in irradiated Bl6/C57 mice (Fig. 22).

Knight-Greenfield et al. from the Mount Sinai School of Medicine (New York, NY), the Rigshospitalet (Copenhagen, Denmark), and the Roswell Park Cancer Center (Buffalo, NY) reported that "Interim FDG PET/CT predicts response and progression-free survival better than baseline clinical

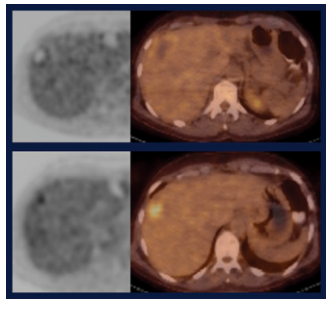

FIGURE 21. PET/CT after radiofrequency ablation of colorectal liver metastases. Top images show rim-shaped uptake adjacent to photopenic radiofrequency ablation zone at 3 months. Bottom images show focal uptake at 6 months, which is highly suggestive of local-site recurrence.

and metabolic parameters in Hodgkin lymphoma: correlation with various methodologies" [69]. They found that a variety of quantitative parameters, including PERCIST, appeared to predict outcome better than a range of qualitative and traditional quantitative criteria.

Size does still matter in Hodgkin lymphoma. Kobe et al. from the University Hospital of Cologne (Germany) reported that "Relative reduction of residual tumor improves outcome prediction of PET after effective chemotherapy for patients with advanced stage Hodgkin lymphoma" [178]. The researchers showed that patients in whom tumor size did not diminish by at least 40% in treatment fared worse in progression-free survival, indicating that relative tumor size can be used for prognostic differentiation in PET-positive patients

Sachpekidis et al. from the German Cancer Research Center (Heidelberg, Germany) and University Hospital Heidelberg (Germany) reported on "Dynamic FDG PET-CT in stage IV melanoma patients following ipilimumab therapy" [1606]. Ipilimumab is newly FDA approved, and assessment of response is quite challenging. These authors found that ^{18}F-FDG PET/CT was quite sensitive in detecting changes during treatment. They also found that, in terms of therapy response evaluation, the number of metastatic lesions detected was a more important factor than SUV changes during the course of treatment. They concluded that in clinical practice PET/CT could be performed as a baseline study and at the end of ipilimumab therapy for treatment response evaluation.

Therapeutic Guidance, Dosimetry, and Radiopharmaceutical Therapy

Among therapeutic isotopes described at this meeting, ^{90}Y predominated, with ^{131}I a distant second and additional presentations on ^{188}Re, ^{211}At, ^{223}Ra, and ^{212}Pb. Several groups reported on combining radiosensitization and radioisotope therapy. Morgenroth et al. from the University of Aachen (Germany) reported on "Breaking dormancy of cancer stem cells: 2-step strategy for killing of cancer stem cell subpopulation of multiple myeloma" [452]. Tesson et al. from the University of Glasgow (Scotland), Molecular Insight Pharmaceuticals (Cambridge, MA), and Progenics Pharmaceuticals (Tarrytown, NY) reported on "Enhancement of prostate-targeted radiotherapy using ^{131}I-MIP-1095 in combination with radiosensitizing chemotherapeutic drugs" [119].

Hino et al. from FUJIFILM RI Pharma Co., Ltd. (Chiba, Japan), and Perseus Proteomics Inc. (Tokyo, Japan) reported on "Preclinical evaluation of anti-cadherin-3 mouse-human chimeric monoclonal antibody FF-21101 radioimmunotherapy" [1367]. The investigators described the anticancer effect and safety of ^{90}Y-DOTA-FF-21101 in animals (Fig. 23). Their results are encouraging, although the translation to human studies will require significant additional investigation.

Tann et al. from the Indiana University Hospital (Indianapolis) reported on "PET/CT dosimetric mapping of ^{90}Y therasphere biodistribution following radioembolization for hepatocellular cancer" [12]. The group produced Medical Internal Radiation Dose voxel-based S-value dose maps that provided accurate quantification and localization of absorbed dose, with presumed correlations with outcomes, although more study is needed (Fig. 24).

Fendler et al. from the Ludwig-Maximilians-University of Munich (Germany) reported on a "Nomogram including pretherapeutic parameters for prediction of survival after selective internal radiation therapy of hepatic metastases from colorectal cancer" [1386]. The group proposed a practical model for 1-year survival after radioembolization in patients with liver metastases from colorectal cancer.

Konijnenberg et al. from Erasmus MC (Rotterdam, The Netherlands) reported on "Dose-effect model for volume reduction of spleen after peptide receptor radionuclide therapy with ^{177}Lu-DOTA-octreotate" [584]. These investigators correlated tumor shrinkage with dose delivered. Dewaraja et al. from the University of Michigan Medical School (Ann Arbor) reported that "Tumor absorbed dose predicts progression-free survival following ^{131}I radioimmunotherapy" [51]. This group looked at radioimmunotherapy with anti-CD20 and found that those receiving ^{131}I-tositumomab absorbed radiation doses $>$200 cGy had the best outcomes. These results suggest that the tumor absorbed dose, which can be predicted from a tracer study, can potentially be used to customize ^{131}I radioimmunotherapy protocols.

Shimoni et al. from Chaim Sheba Medical Center (Tel-Hashomer, Israel) and a consortium of Israeli medical centers reported on "A comparative multicenter study of ^{90}Y-ibritumomab tiuxetan with high-dose BEAM chemotherapy versus BEAM alone prior to autologous stem-cell transplantation in patients with aggressive lymphoma" [115]. In this study, Zevalin plus chemotherapy produced better results than che-

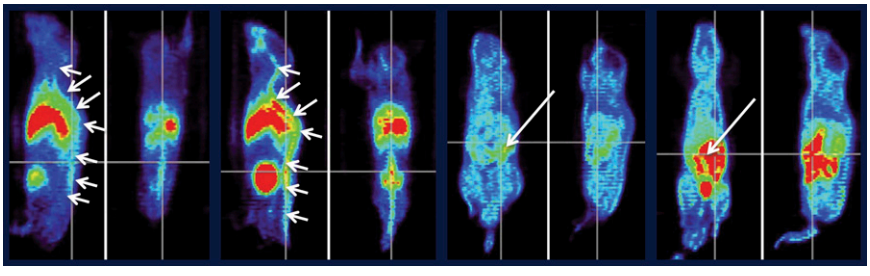

FIGURE 22. Molecular imaging after external irradiation. Left 4 images: sagittal and coronal ^{64}Ga-NODA-GA-annexin V images in bone marrow at day 3 in sham-irradiated (left 2 images, 0 Gy) and total-body-irradiated (right 2 images, 8 Gy) mice. Right 4 images: Sagittal and coronal ^{18}F-FLT images in the gastrointestinal tract at day 3 in sham-irradiated (left 2 images, 0 Gy) and total-body-irradiated (right 2 images, 8 Gy) mice.

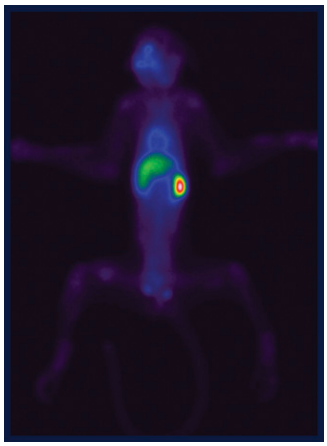

FIGURE 23. Anticancer effect and safety of ^{90}Y DOTA-FF-21101. Biodistribution of ^{111}In-DOTA-FF in male cynomolgus money 72 h after administration.

motherapy alone. The concept of consolidation was advanced by Kraeber-Bodere et al. from CHU/ICO/Inserm (Nantes, France) and a consortium of French and U.S. investigators, who reported on "Consolidation anti-CD22 fractionated radioimmunotherapy with ^{90}Y-epratuzumab tetraxetan following R-CHOP in elderly diffuse large B-cell lymphoma patient" [179]. In this study, some patients were converted by RIT to a complete response after achieving a partial response with chemoimmunotherapy.

Ezziddin et al. from the University of Bonn (Germany) and a consortium of German universities and medical centers reported on "Peptide receptor radionuclide therapy for neuroendocrine neoplasms in Germany: a multi-institutional registry study with prospective follow up on 450 patients" [579]. In this large-cohort research, peptide receptor radionuclide therapy was found to be both effective and safe.

Kesner et al. from Hadassah University Hospital (Jerusalem, Israel) reported on "Radiation dosimetry in ^{177}Lu-DOTATATE therapy: inter- and intrapatient variability" [1376]. These investigators found that variation among tumor and organ doses was high, both on an inter- and intrapatient basis, so that patient-specific and cycle-specific dosimetry remain important.

Flamen et al. from the Institut Jules Bordet (Brussels, Belgium), Weston Park Hospital (Sheffield, UK), Oslo University Hospital (Norway), CHU Sart Tilman (Liège, Belgium), and Algeta ASA (Oslo, Norway) reported on "^{18}F-FDG PET: changes in uptake as a method to assess ^{223}Ra-dichloride response in bone metastases of breast cancer patients with bone-dominant disease" [647]. ^{223}Ra-dichloride has recently been approved in the United States. These researchers showed the utility of ^{18}F-FDG PET in assessing early response (Fig. 25).

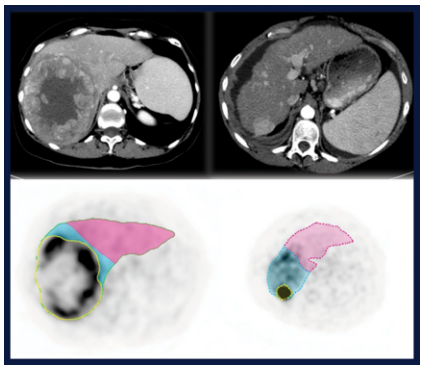

FIGURE 24. PET/CT dosimetric mapping of ^{90}Y therasphere distribution after radioembolization for hepatocellular cancer. Left: ^{90}Y PET/CT acquired in patient after radioembolization (top) and dosimetric map (bottom) indicating a dose of 132 Gy to the lesion and 34 Gy to parenchyma. Right: Corresponding images in a second patient, with dosimetric mapping indicating a dose of 300 Gy to the lesion and 123 Gy to parenchyma.

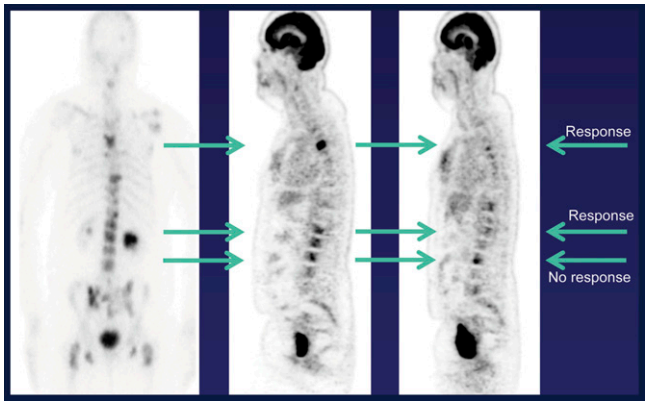

FIGURE 25. ^{18}F-FDG PET/CT and ^{223}Ra therapy. Left: baseline bone scan. Middle: baseline ^{18}F-FDG PET image. Right: ^{18}F-FDG PET acquired after 2 injections of ^{223}Ra showed a significant decrease (>25% decrease in SUVmax) in tracer uptake intensity in multiple, though not all, bone metastases located in the thoracic and lumbar spine, indicating a partial metabolic treatment response in several tumor foci early in ^{223}Ra therapy.

Summary

As we have seen, oncology presentations at the SNMMI 2013 Annual Meeting were dominated by PET, with ^{18}F-FDG remaining the most frequently used tracer. We have seen a clear trend toward personalized and standardized quantitative in vivo phenotyping. Therapy is a growing focus of interest. Improving patient outcomes—and documenting such improvement—must remain a central focus of our scientific and clinical work.

ACKNOWLEDGMENTS

I would like to thank Julia Buchanan at Johns Hopkins for her helpful review and advice in preparation of this presentation, as well as Harvey Ziessman, MD, Zsolt Szabo, MD, PhD, Steve Cho, MD, Rathan Subramaniam, MD, PhD, and our Hopkins residents and fellows for their critical insights. This presentation would not be complete without recognizing the late Henry N. Wagner, Jr., MD, for his superb service over 3 decades in providing a comprehensive review of SNM meetings. He remains a role model for all of our current Highlights presenters.

Richard L. Wahl, MD
Johns Hopkins Medicine
Baltimore, MD